The electrochemical ion-transfer reactivity of porphyrinato metal complexes in 4-(3-phenylpropyl)pyridine | water systems

Michael J. Bonné,[a] Christopher Reynolds,[a] Stuart Yates,[a] Galyna Shul,[b] Joanna Niedziolka,[b] Marcin Opallo[b] and Frank Marken*[a]

Received (in Durham, UK) 10th October 2005, Accepted 23rd January 2006
First published as an Advance Article on the web 6th February 2006
DOI: 10.1039/b514348a

The transfer of ions between an aqueous and an organic phase is driven electrochemically at a triple phase junction graphite | 4-(3-phenylpropyl)pyridine | aqueous electrolyte. Tetraphenylporphyrinato (TPP) metal complexes ($MnTPP^+$, $FeTPP^+$, CoTPP) and hemin readily dissolve in the organic 4-(3-phenylpropyl)pyridine phase and undergo oxidation/reduction processes which are coupled to liquid | liquid ion transfer. In order to maintain charge neutrality, each one-electron oxidation (reduction) process is coupled to the transfer of one anion (here PF_6^-, ClO_4^-, SCN^-, NO_3^-, OCN^-, or CN^-) from the aqueous (organic) into the organic (aqueous) phase. The range of anions studied allows effects of hydrophobicity and complex formation (association of the anion to the metal center) to be explored. A preliminary kinetic scheme is developed to quantify complex formation, facilitated anion transfer, and competing cation transfer processes. The effects of the organic solvent on the ion transfer processes are explored. Very strong binding and specific effects are observed for the reversible cyanide transfer process.

1. Introduction

The study of ion transfer between two immiscible liquid phases is of considerable importance in biological, physiological, ion extraction, sensing, and phase transfer technology contexts.[1,2] There has been interest in electrochemical methods designed to directly measure the transfer of ions as a function of an applied potential across the liquid | liquid interface.[3] Techniques based on cyclic voltammetry at macro- and micro-interfaces,[4,5] steady state microprobe voltammetry,[6] and hydrodynamic voltammetry[7,8] are known. Recently, new types of ion transfer processes photochemically driven[9] and in zeolitic membranes[10] and processes involving direct liquid | liquid interfacial electron transfer[11,12] have been reported. Novel types of electroorganic processes based on two phase electrolysis have been explored.[13] Usually, supporting electrolytes are added into both the organic and the aqueous phase to ensure sufficient electrical conductivity for the liquid | liquid interface to be polarized. However, in some cases it can be beneficial to avoid the use of supporting electrolyte in the organic phase, for example to avoid interference from electrolyte ion transfer[14] or in cases where the solubility of ions in the organic phase is low (*e.g.* for processes in silicon oil or alkanes[15,16]). A novel methodology avoiding the use of supporting electrolyte is exploiting the fact that ion transfer processes also occur at triple phase boundaries.[17]

Traditionally, a liquid | liquid system composed of a phase α and a phase β has been studied by placing an electrode into the bulk liquid [see Fig. 1(A)]. In elegant and pioneering experimental work Anson *et al.*[18–20] have demonstrated the use of thin films of organic liquids at electrode surfaces. Alternatively, when the electrode is placed directly at the liquid | liquid interface [see Fig. 1(B)], the triple phase boundary can be accessed and processes measured even in the absence of intentionally added supporting electrolyte in phase α. This kind of process was further exploited with mesoporous electrodes,[21,22] rod shaped electrodes,[23] single droplets,[24] or arrays of microdroplets.[25] Depending on whether the transfer of ions from the aqueous phase induces more ionic conductivity in the organic phase, characteristic changes in the detected currents are observed.[26]

In this study the electrochemical and ion transfer reactivity are surveyed for a range of porphyrinato metal complexes (see Fig. 2) dissolved in 4-(3-phenylpropyl)pyridine, deposited in the form of an array of microdroplets onto basal plane pyrolytic graphite, and in contact with aqueous solutions.

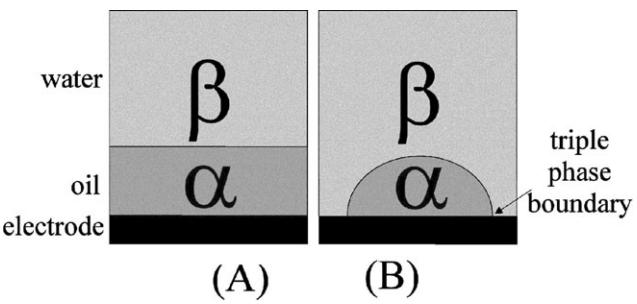

Fig. 1 Schematic diagram showing (**A**) a conventional liquid | liquid interface and (**B**) a liquid | liquid | solid interface, forming a triple phase boundary.

[a] *Department of Chemistry, University of Bath, Claverton Down, Bath, UK BA2 7AY. E-mail: F.Marken@bath.ac.uk*
[b] *Institute of Physical Chemistry, Polish Academy of Sciences, ul. Kasprzaka 44/52, 01-224 Warszawa, Poland*

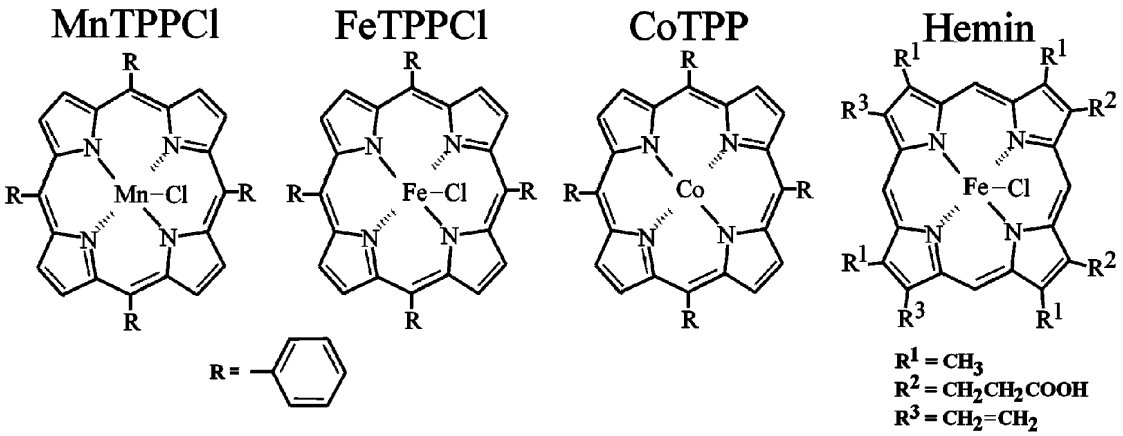

Fig. 2 Chemical formulae of metalloporphyrins, 5,10,15,20-tetraphenyl-21*H*,23*H*-porphine manganese(III) chloride (MnTPPCl) 5,10,15,20-tetraphenyl-21*H*,23*H*-porphine iron(III) chloride (FeTPPCl), 5,10,15,20-tetraphenyl-21*H*,23*H*-porphine cobalt(II) (CoTPP), and protoporphyrin-IX Fe(III) chloride (hemin).

Transfer of anions is observed for PF_6^-, ClO_4^-, SCN^-, NO_3^-, OCN^-, and for CN^- and the midpoint potential for the transfer process is analyzed in terms of both the Gibbs energy of ion transfer from aqueous to organic media and metal–anion association processes.

Porphyrinato-type metal complexes have previously been employed in liquid | liquid electrochemical studies to investigate the ion transfer kinetics[27] and the transfer of cations.[28] We have demonstrated the ion transfer electrochemistry for CoTPP[29] and for MnTPP[30] immobilized within 4-(3-phenylpropyl)pyridine on basal plane pyrolytic graphite and within mesoporous platinum electrodes, respectively. There is a general interest in the chemistry and versatile electrochemistry of the family of porphyrinato metal complexes[31] which are abundant in nature[32] and which may serve as catalysts for example in oxygenation[33] or oxygen reduction processes.[34] In the solvent system studied here, 4-(3-phenylpropyl)pyridine, porphyrinato metal complexes are readily soluble due to the favorable interaction of the pyridine nucleophile with the metal center.[35] Solvent binding with one or two axial 4-(3-phenylpropyl)pyridine ligands is likely to dominate the behaviour of the metal centers in the solution phase, although fluxional behaviour, substitution and specific binding to anions, in particular strongly binding anions such as cyanide, is possible. In this study, the transfer and binding of anions to porphyrinato metal complexes is investigated systematically. It is shown that only for the weakly coordinating anions such as PF_6^-, ClO_4^-, SCN^-, and NO_3^- simple anion transfer occurs. For OCN^- and CN^- facilitated ion transfer occurs and order of magnitude estimates for the corresponding binding constants are obtained. The cyanide anion gives a special "signature response" (a second oxidation step) when transferred in the presence of 5,10,15,20-tetraphenyl-21*H*,23*H*-porphyrinato manganese(III).

2. Experimental

2.1. Chemical reagents

Chemical reagents were purchased from Aldrich and used without further purification. Solvent systems studied were 3-(4-phenylpropyl)pyridine (PPP), 2-nitrophenyl octyl ether (NPOE), 4-nitrophenyl nonyl ether (NPNE), and nitrobenzene (NB). Solutions were prepared in 4-(3-phenylpropyl)pyridine (or other solvents) by dissolving (with gentle heating) 5,10,15,20-tetraphenyl-21*H*,23*H*-porphine iron(III) chloride (FeTPPCl, 70 mM), 5,10,15,20-tetraphenyl-21*H*,23*H*-porphine cobalt(II) (CoTPP, 53 mM), 5,10,15,20-tetraphenyl-21*H*,23*H*-porphine manganese(III) chloride (MnTPPCl, 67 mM), or hemin (78 mM). Next, 100 mg of the solution was added into 10 mL acetonitrile (HPLC grade, Aldrich) to provide a deposition solution. Typically 5–10 μL of the deposition solution was placed onto the basal plane pyrolytic graphite electrode surface and after evaporation of the acetonitrile phase an electrochemically active microdroplet deposit remained.[36] Fresh solutions were prepared for each set of experiments due to slow precipitation of solids in acetonitrile. Only MnTPP resulted in stable deposition solutions and therefore MnTPP was chosen as the redox system for the comparison of different types of organic solvents. Demineralized water was taken from an Elgastat filter system (Elga, Bucks, UK) with a resistivity of not less than 15 MΩ cm and was used to prepare aqueous 0.1 M electrolyte solutions of $NaClO_4$, NaSCN, $NaNO_3$, KPF_6, KOCN, KCN, KCl, KI, or NaBr.

2.2. Instrumentation

Voltammetric measurements were conducted with a μ-Autolab II potentiostat system (Eco Chemie, The Netherlands) in a conventional three-electrode electrochemical cell. Experiments were performed in staircase voltammetry mode with platinum gauze counter and saturated calomel reference electrode (SCE, REF401, Radiometer). The working electrode was a 4.9 mm diameter basal plane pyrolytic graphite electrode (Pyrocarbon, Le Carbone, UK). The graphite electrode surface was renewed by polishing on a fine silicone carbide paper (P1200, Buehler) and removal of excess graphite flakes prior to each use. Aqueous solutions were thoroughly de-aerated with argon (BOC) prior to conducting experiments, at a temperature of 22 ± 2 °C.

3. Results and discussion

3.1. Electrochemically driven ion transfer across the 4-(3-phenylpropyl)pyridine | aqueous electrolyte interfaces

4-(3-Phenylpropyl)pyridine (PPP) as a highly water insoluble but coordinating solvent allows metal complexes such as tetraphenylporphyrinato complexes of Mn, Fe, and Co to be readily dissolved. The resulting solutions show electrochemical reactivity similar to solutions in pyridine.[35] In order to deposit small quantities of these metal complex solutions in the form of microdroplets onto basal plane pyrolytic graphite (BPPG) electrodes, a solvent evaporation approach employing acetonitrile has been employed (see Experimental). Fig. 3 shows typical voltammograms obtained with porphyrinato complexes of Mn, Fe, and Co.

The voltammetric response for the FeTPP metal complex is observed with a midpoint potential of 0.04 *vs.* SCE and is consistent with a highly reversible redox system in close contact with the electrode surface (diffusion processes are too fast to significantly affect the voltammetric response). The initial open circuit potential of 0.2 V *vs.* SCE is consistent with the Fe(III) state of the starting material and the overall redox process may be described as shown in eqn (1).

$$FeTPPL_2^+(org) + X^-(org) + e^- \rightleftarrows FeTPPL_2(org) + X^-(aq) \quad (1)$$

The metal centered reduction Fe(III/II) in $FeTPPL_2$ [L = 4-(3-phenylpropyl)pyridine] is accompanied by the transfer of the counter anion, here $X^- = PF_6^-$, from the organic PPP phase into the aqueous 0.1 M KPF_6 phase. This process can be verified by comparison with the behaviour of other anions (each anion contributes to a distinct shift in the midpoint potential at which this process is observed) but is in contrast to an earlier report of cation transfer into nitrobenzene accompanying the Fe(III/II) process.[28] However, in the earlier study nitrobenzene, a weaker donor solvent, was employed and here the presence of the 3-(4-phenylpropyl)pyridine ligands is clearly changing the ability of the FeTPP metal complex to bind chloride. Therefore the anion transfer process is favoured over cation transfer as will be shown in more detail below.

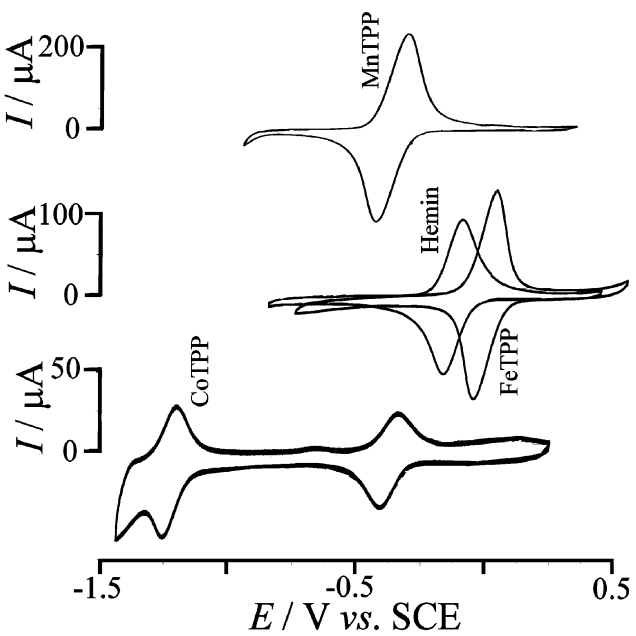

Fig. 3 Cyclic voltammograms (scan rate 0.1 V s^{-1}) for the oxidation/reduction of a 50 μg deposit of a solution of MnTPP (67 mM), hemin (78 mM), FeTPP (70 mM), and CoTPP (53 mM) in PPP, immobilized onto a 4.9 mm diameter basal plane pyrolytic graphite electrode, and immersed in aqueous 0.1 M KPF_6.

A second porphyrinato Fe complex, hemin (see Fig. 2), shows characteristics similar to those observed for FeTPP. A reversible Fe(III/II) system associated with anion transfer is observed at a midpoint potential of −0.13 V *vs.* SCE (see Fig. 3). The shift in potential of 170 mV to more negative potentials when compared to FeTPP is believed to be due to the (more electron-rich) electronic characteristics of the protoporphyrinato-IX ligand.

The electrochemical reduction of $MnTPPL_2^+$ is observed at a midpoint potential of −0.37 V *vs.* SCE (see Fig. 3). The initial open circuit potential of −0.05 V *vs.* SCE is consistent with a Mn(III/II) redox process and the following process is believed to occur [eqn (2)].

$$MnTPPL_2^+(org) + X^-(org) + e^- \rightleftarrows MnTPPL_2(org) + X^-(aq) \quad (2)$$

The transfer of the anion between the organic and the aqueous phase is occurring very rapidly and is again coupled reversibly to the electron transfer process (*vide infra*). It is interesting to note the magnitude of the voltammetric signal in comparison to the smaller voltammetric responses observed for the other metal complexes. The MnTPP complex is highly soluble in the organic phase even in the presence of acetonitrile and appears to be most effectively deposited and converted under the conditions employed here.

Next, the voltammetric responses for the CoTPP metal complex system were investigated.[29] The reversible voltammetric response for the Co(III/II) redox system is observed with a midpoint potential of −0.38 V *vs.* SCE (see Fig. 3). This process has been identified previously[29] as an anion transfer process [eqn (3)].

$$CoTPPL_2^+(org) + X^-(org) + e^- \rightleftarrows CoTPPL_2(org) + X^-(aq) \quad (3)$$

For the CoTPP system also the second metal centered reduction Co(II/I) is observed at a midpoint potential of −1.23 V *vs.* SCE (see Fig. 3). In order to maintain charge neutrality in the organic phase, this reduction process must be coupled to the transfer of cations, here $C^+ = K^+$, from the aqueous phase into the organic phase [eqn (4)].

$$CoTPPL_2(org) + C^+(aq) + e^- \rightleftarrows CoTPPL_2^-(org) + C^+(org) \quad (4)$$

In the presence of 0.1 M KPF_6 the potassium cation is crossing the aqueous | organic interface and is solvated in the 4-(3-phenylpropyl)pyridine solvent. The coordination of the

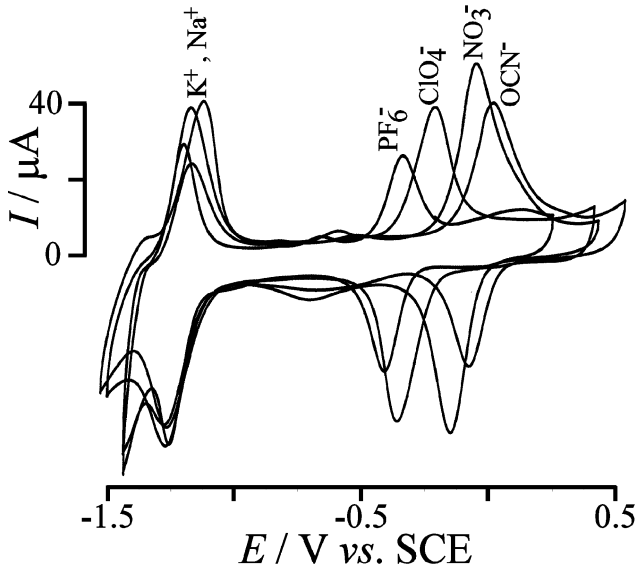

Fig. 4 Cyclic voltammograms (scan rate 0.1 V s^{-1}) for the oxidation/reduction of a 50 μg deposit of a solution of CoTPP (53 mM) in PPP, immobilized onto a 4.9 mm diameter basal plane pyrolytic graphite electrode, and immersed in aqueous 0.1 M solutions of KPF_6, $NaClO_4$, KNO_3, and KOCN.

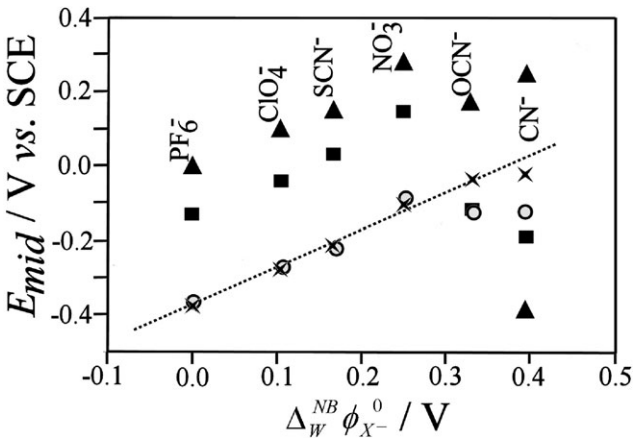

Fig. 5 Plot of midpoint potentials obtained from cyclic voltammograms for the oxidation/reduction of a 50 μg deposit of a solution of MnTPP (circle, 67 mM), hemin (filled squares, 78 mM), FeTPP (filled triangles, 70 mM), and CoTPP (crosses, 53 mM) in PPP, immobilized onto a 4.9 mm diameter basal plane pyrolytic graphite electrode, and immersed in aqueous 0.1 M solutions of KPF_6, $NaClO_4$, KSCN, KNO_3, KOCN, and KCN *versus* the standard membrane potentials at the water | nitrobenzene interface (see literature[37,38]). For cyanate no literature value was available and therefore the standard membrane potential $\Delta_W^{NB}\phi_{X^-}{}^0 = 0.34$ V has been obtained by extrapolation. The dashed line shows the ideal trend for a simple anion transfer process.

pyridine to the cation (here K^+) has a considerable effect on the transfer potential as has been demonstrated.[29]

3.2. The effect of the aqueous electrolyte on the electrochemically driven ion transfer across the 4-(3-phenylpropyl)pyridine | aqueous electrolyte interfaces

Next, the effect of the type of anion on the anion transfer process was studied. Voltammograms have been recorded in a range of aqueous electrolyte solutions and the midpoint potential for the processes can be analyzed. Fig. 4 shows the voltammetric responses obtained for the oxidation and reduction of the CoTPP system in KPF_6, $NaClO_4$, KNO_3, and in KOCN. All Co(II/I) redox processes are superimposed at a midpoint potential of −1.22 V *vs.* SCE which is consistent with the reversible transfer of K^+ (or Na^+ which occurs at the midpoint potential of −1.20 V *vs.* SCE[29]). The voltammetric responses for the Co(III/II) system which are coupled to anion transfer show a distinct shift for each type of anion. This potential shift can be correlated with the tabulated Gibbs energy of transfer for anions in a water | nitrobenzene system.[37] Data for a sequence of anions from PF_6^- (the most hydrophobic anion) to OCN^- (the most hydrophilic anion) emerge and are summarized in Fig. 5.

The plot in Fig. 5 demonstrates the relationship of the midpoint potentials observed in these experiments towards the literature values for the standard membrane potential $\Delta_W^{NB}\phi_{X^-}{}^0$ for a specific anion at the aqueous | nitrobenzene interface. An excellent linear correlation between midpoint potentials and literature transfer potentials is observed and the theoretical dependency for the CoTPP system (crosses) is indicated with a dotted line. Clearly most anions (with the notable exception of CN^-) follow the predicted behaviour and therefore all of these processes are consistent with a simple anion transfer mechanism [see eqn (1)]. The methodology, in particular when using the CoTPP redox system, provides a simple and reliable access to thermodynamic data for the transfer of anions (and cations) from aqueous into organic media. However, very hydrophilic and strongly complexing anions such as cyanate and cyanide appear to result in a

Table 1 Midpoint potential data obtained from cyclic voltammograms (scan rate 0.1 V s^{-1}) for the oxidation and reduction of porphyrinato metal complexes in PPP immobilized in the form of an array of microdroplets on basal plane pyrolytic graphite and immersed in aqueous 0.1 M electrolyte solution

	$E_{mid}(PF_6^-)$/ V *vs.* SCE	$E_{mid}(ClO_4^-)$/ V *vs.* SCE	$E_{mid}(SCN^-)$/V *vs.* SCE	$E_{mid}(NO_3^-)$/V *vs.* SCE	$E_{mid}(OCN^-)$/V *vs.* SCE	ΔE_{mid}/mV[a]	$E_{mid}(CN^-)$/V *vs.* SCE	ΔE_{mid}/mV[a]
FeTPP	0.04	0.10	0.15	0.28	0.17	−124	−0.39	−145
Hemin	−0.13	−0.04	0.03	0.15	−0.12	−300	−0.19	−450
MnTPP	−0.37	−0.28	−0.23	−0.09	−0.12	−90	−0.12	−200
CoTPP	−0.38	−0.28	−0.21	−0.10	−0.03	≈0	−0.02	≈0[b]

[a] The value ΔE_{mid} corresponds to the potential gap between the measured reversible (or midpoint) potential and the predicted "ideal" value for cyanate and cyanide anions. [b] For the CoTPP system in the presence of cyanide the position of the oxidation peak is not affected by binding to cyanide due to slow kinetics.

different reaction pathway in particular for metal porphyrinato complexes other than CoTPP. The resulting shift in reversible potential (see Table 1) may be employed to obtain an estimate of the binding ability of the metal complex towards the transferred anion (*vide infra*).

3.3. The transfer of strongly coordinating anions across the 4-(3-phenylpropyl)pyridine | aqueous electrolyte interfaces: cyanate

The transfer of some types of anion results in voltammetric responses which are inconsistent with the simple ion transfer mechanism and is more complex *e.g.* involving more than one current peak. For the cyanate anion transfer, CoTPP shows two voltammetric responses which are consistent with a simple anion transfer (see Fig. 6). Both the Co(III/II) and the Co(II/I) redox systems are observed at the predicted potentials (see Fig. 5).

However, the Fe(III/II) voltammetric response for the FeTPP complex is changed into a chemically irreversible response with two distinct reduction peaks (see Fig. 6). Reducing the scan rate to 10 mV s^{-1} results in the peak at *ca.* 0.1 V *vs.* SCE to dominate and the second reduction peak at *ca.* −0.4 V *vs.* SCE disappears (*vide infra*). Therefore the reduction peak at more negative potentials must be due to an intermediate with a reduction potential shifted to more negative potentials. The formation of an adduct between the metal center and the anion after oxidation [see eqn (5)] is most likely.

$$FeTPPL_2^+(org) + X^-(org) \rightleftarrows FeTPPLX(org) + L \quad (5)$$

This ligand exchange equilibrium process appears to be relatively fast and therefore only with sufficiently fast scan rates can the adduct, FeTPPLX(org), be detected directly. The shift of the midpoint potential ΔE_{mid} for the anion transfer process

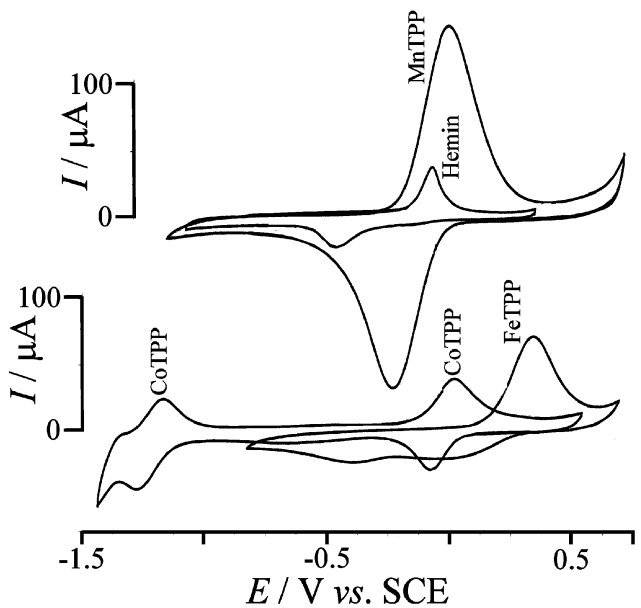

Fig. 6 Cyclic voltammograms (scan rate 0.1 V s^{-1}) for the oxidation/reduction of a 50 μg deposit of a solution of MnTPP (67 mM), hemin (78 mM), FeTPP (70 mM), and CoTPP (53 mM) in PPP, immobilized onto a 4.9 mm diameter basal plane pyrolytic graphite electrode, and immersed in aqueous 0.1 M KOCN.

(see Table 1) is a tell-tale sign for the equilibration process. An estimate for the apparent equilibrium constant K_{eq}^{ox} for the adduct formation can be obtained [eqn (6)].

$$K_{eq}^{ox} = \frac{[M(III)TPPLX][L]}{[M(III)TPPL_2^+][X^-]} = \exp\left(-\frac{F}{RT}\Delta E_{mid}\right) \quad (6)$$

In this equation the complementary equilibrium for the reduced M(II)TPP system has been ignored for clarity. From the data in Table 1 and for the $FeTPP^+$–cyanate interaction the apparent equilibrium constant $K_{eq}^{ox} = 100$ is obtained. It is interesting to consider the nature of the second reduction peak observed at −0.4 V *vs.* SCE (see Fig. 6). In order to maintain charge neutrality, this process has to be associated with the transfer of cations from the aqueous phase into the organic phase [eqn (7)].

$$FeTPPLX(org) + C^+(aq) + e^- \rightleftarrows FeTPPLX^-(org) + C^+(org) \quad (7)$$

This type of cation transfer process was previously observed for the FeTPPCl system in nitrobenzene solution and employed for the investigation of thermodynamic parameters for liquid | liquid cation transfer.[28]

The voltammetric response for hemin in the presence of cyanate is similar to that observed for FeTPP. However, the scan rate required to allow both reduction responses to be observed simultaneously is considerably lower. The apparent equilibrium constant can be estimated as $K_{eq}^{ox} = 10^5$ (see Table 1). For the MnTPP complex only a small shift in the midpoint potential is observed, possibly indicating the formation of a weaker complex, MnTPPLX(org) with $K_{eq}^{ox} = 30$. However, for the quantitative analysis/comparison of binding constants the apparent equilibrium constant K_{eq}^{red} for the $MnTPPLX^-$(org) complex is also required (*vide infra*).

3.4. The transfer of strongly coordinating anions across the 4-(3-phenylpropyl)pyridine | aqueous electrolyte interfaces: cyanide

Next, the much more strongly binding cyanide anion was investigated. The oxidation of CoTPP is now associated with a chemically irreversible Co(III/II) process. The oxidation peak at 0.02 V *vs.* SCE is close to the potential predicted for a simple anion transfer. However, the corresponding reduction peak is shifted to much more negative potentials and split at −0.65 V and at −1.15 V *vs.* SCE (see Fig. 7). The Co(II/I) process is observed at the correct potential and appears not to be affected. Therefore the formation of the CoTPPLCN(org) adduct appears to be overall chemically reversible.

The voltammetric response for the FeTPP metal complex in the presence of cyanide is dramatically changed compared to that expected for a simple anion transfer (Fig. 7). A new voltammetric response is observed at −0.39 V *vs.* SCE which is 0.78 V more negative compared to the response predicted for simple anion transfer. A small second oxidation peak at 0.25 V *vs.* SCE (not shown in Fig. 7) indicates the presence of two Fe(II) metal complexes which are very likely to be $FeTPPLCN^-$(org) and $FeTPPL_2$(org). That is, for the FeTPP system the equilibrium is shifted towards adduct formation already in the Fe(II) state. For the $FeTPPL_2$(org) oxidation an

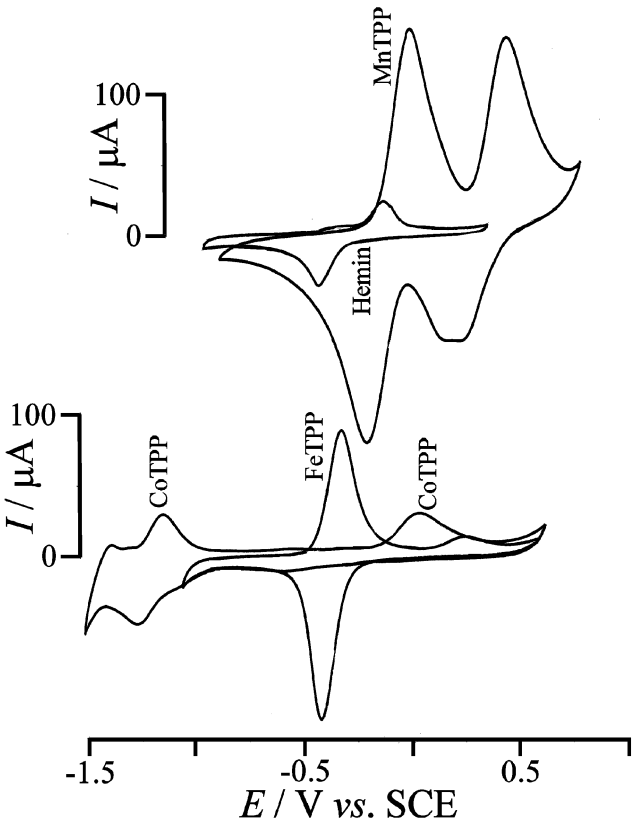

Fig. 7 Cyclic voltammograms (scan rate 0.1 V s^{-1}) for the oxidation/reduction of a 50 μg deposit of a solution of MnTPP (67 mM), hemin (78 mM), FeTPP (70 mM), and CoTPP (53 mM) in PPP, immobilized onto a 4.9 mm diameter basal plane pyrolytic graphite electrode, and immersed in aqueous 0.1 M KCN.

apparent binding constant of $K_{eq}^{ox} = 300$ can be estimated. However, the proposed formation of $FeTPPLCN^-$(org) requires a new type of equilibrium involving the transfer of both CN^- and K^+ simultaneously from the aqueous phase into the organic phase [eqn (8)].

$$FeTPPL_2(org) + CN^-(aq) + K^+(aq) \rightleftarrows FeTPPLCN^-(org) + K^+(org) + L \quad (8)$$

The apparent equilibrium constant for this process, K_{eq}^{red}, may be expressed similarly to K_{eq}^{ox}, but due to insufficient experimental data this additional equilibrium constant is currently not directly accessible (*vide infra*). Furthermore, the two-phase nature of the equilibrium process requires the equilibrium constants for the partitioning of CN^- and K^+ to be introduced in order to adequately describe the overall equilibrium process.

For hemin in the presence of CN^-, a voltammetric signal very similar to that observed in OCN^- is observed (see Fig. 7) and the fast and reversible formation of an adduct is proposed with $K_{eq}^{ox} = 10^7$ (see Table 1). It appears likely that the cyanide binding is stronger and the exchange of ligands is faster for the hemin complex when compared with the FeTPP complex. However, under the conditions employed here, the reduced form of hemin does not have the ability to extract KCN directly from the aqueous solution and the comparison of K_{eq}^{ox} values may be misleading without taking into consideration K_{eq}^{red} values (*vide infra*).

The MnTPP metal complex shows clear evidence for cyanide binding associated with the M(III/II) oxidation process. The shift of the midpoint potential may be attributed to the fast and reversible association process [eqn (9)] and formation of an adduct with $K_{eq}^{ox} = 2400$ (see Table 1). Perhaps surprisingly, a second oxidation process is observed with essentially the same peak current. This process is tentatively assigned to a second oxidation with transfer of cyanide [eqn (10)].

$$Mn(II)TPPL_2(org) + CN^-(aq) \rightleftarrows Mn(III)TPPLCN(org) + e^- + L \quad (9)$$

$$Mn(III)TPPLCN(org) + CN^-(aq) \rightleftarrows Mn(IV)TPP(CN)_2(org) + e^- + L \quad (10)$$

3.5. The transfer of anions across the 4-(3-phenylpropyl)pyridine | aqueous electrolyte interfaces: solvent effects

It is interesting to explore the effect of the organic solvent environment on the reactivity of the porphyrinato metal complex and on the ion transfer process. It has been pointed out that the ability of the 3-(4-phenylpropyl)pyridine solvent to directly bind to the metal center is governing the solubility and reactivity of the metal complexes. Experiments were conducted in 3-(4-phenylpropyl)pyridine, nitrobenzene, 2-nitrophenyl octyl ether, and 4-nitrophenyl nonyl ether for the MnTPP redox system. The anion transfer process consistent with data presented in Fig. 5 was observed in all cases (see Table 2). However, often a second process was observed at potentials *ca.* 0.25 V negative to the anion transfer process (see Fig. 8).

Fig. 8 shows typical voltammograms obtained with microdroplets of nitrobenzene immobilized onto a basal plane pyrolytic graphite electrode and immersed in aqueous solutions containing chloride, bromide, or iodide. The anion

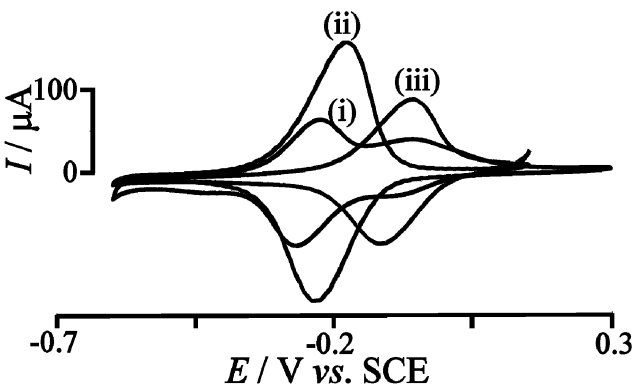

Fig. 8 Cyclic voltammograms (scan rate 0.05 V s^{-1}) for the oxidation/reduction of a 100 μg deposit of a solution of MnTPP (70 mM) in nitrobenzene, immobilized onto a 4.9 mm diameter basal plane pyrolytic graphite electrode, and immersed in aqueous 0.1 M solutions of (i) KCl, (ii) KI, and (iii) NaBr.

Table 2 Data from cyclic voltammograms (scan rate 50 mV s^{-1}) obtained for solvent microdroplets containing *ca.* 70 mM MnTPP immobilized onto a basal plane pyrolytic graphite electrode and immersed in aqueous 0.1 M KCl, NaBr or KI. The midpoint potentials for the anion transfer (obtained as the potential in the center of oxidation and reduction peaks) and for the cation transfer (in brackets) processes are given

	$\Delta_W^{NB}\phi_{X^-}{}^0$/V[a]	E_{mid}[b] E/V *vs.* SCE	E_{mid} (NB) E/V *vs.* SCE	E_{mid} (NPOE) E/V *vs.* SCE	E_{mid} (NPNE) E/V *vs.* SCE	E_{mid} (PPP) E/V *vs.* SCE
Cl^-	−0.36	−0.01	−0.075 (−0.247)	−0.068 (−0.216)	0.013 (−0.226)	−0.002 (−0.254)
Br^-	−0.30	−0.08	−0.091	−0.071 (−0.236)	−0.004 (−0.249)	−0.051 (−0.244)[c]
I^-	−0.19	−0.18	−0.207	−0.130 (−0.271)	−0.096	−0.179

[a] Obtained from the literature.[37] [b] Obtained by extrapolation from Fig. 5 (for the MnTPP redox system). [c] Obtained from voltammetric responses during initial potential cycles.

transfer responses are consistent with eqn (11) and reversible potential data obtained in different solvent systems are summarized in Table 2.

$$MnTPPL_2(org) + X^-(aq) \rightleftarrows MnTPPL_2{}^+(org) + X^-(org) + e^- \quad (11)$$

The cyclic voltammogram obtained in the presence of aqueous chloride [see Fig. 8, curve (i)] clearly shows a second reversible response (at more negative potentials) which can be identified as the corresponding cation transfer process [eqn (12)].

$$MnTPPLX^-(org) + K^+(org) \rightleftarrows MnTPPLX(org) + K^+(aq) + e^- \quad (12)$$

From data in Table 2 it can be seen that the trends for different solvents are consistent and each solvent has minor effects on the reversible potential data. Experimental data for the midpoint potentials are in agreement with predictions based on literature data and the plot in Fig. 5.

3.6. Numerical simulation of voltammetric data

In order to further interpret results obtained by cyclic voltammetry and to confirm the mechanism, a preliminary and oversimplified mechanistic model was chosen for analysis. The Digisim™ simulation package[39] was employed to generate numerical data. The voltammetric responses observed for the oxidation of porphyrinato metal complexes dissolved in 4-(3-phenylpropyl)pyridine show typical characteristics for processes in a finite diffusion space (here the microdroplet deposit). However, many of the observed voltammograms show broadened and more complex shapes due to droplet size effects and in some cases chemical processes which are coupled to the electron transfer. Here, only a general model to describe the chemical processes is proposed without dealing with non-ideal behaviour.

In most cases only a reversible transfer of an anion X^- from the aqueous phase into the organic phase is coupled to the electrochemical oxidation of the metal complex in the organic phase. However, for more strongly coordinating anions such as cyanate and cyanide an additional complication of the voltammetric response due to homogeneous reaction steps is observed. The homogeneous reaction is proposed to involve binding of the cyanate or cyanide anion directly to the metal center of the metal porphyrin complex. A typical case is shown in Fig. 9 for the oxidation of FeTPP accompanied by transfer of OCN^- from the aqueous to the organic phase. At a scan rate of 100 mV s^{-1} a single oxidation peak and two broad reduction peaks are observed experimentally [see Fig. 9(A)]. At a slower scan rate of 20 mV s^{-1} only one broad reduction response remains.

This behaviour is characteristic for an ion association process (see Fig. 10) where the anion binds to the metal complex thereby replacing a solvent molecule in the ligand sphere. In a simple numerical model this effect can be reproduced (not taking into account residual diffusion, electron transfer kinetic, and resistance effects). Fig. 9(B)(i) shows a

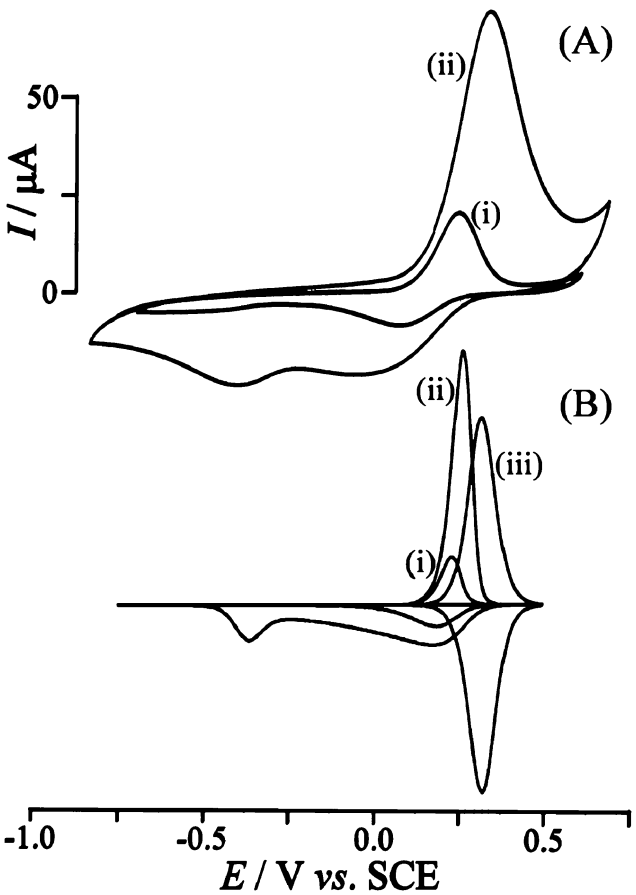

Fig. 9 Experimental (A) and simulated (B) cyclic voltammograms [scan rate (i) 0.02 V s^{-1}, (ii, iii) 0.1 V s^{-1}] for the oxidation/reduction of a 50 μg deposit of a solution of FeTPP (70 mM) in PPP, immobilized onto a 4.9 mm diameter basal plane pyrolytic graphite electrode, and immersed in aqueous 0.1 M KOCN. Simulation parameters were chosen consistent with a finite space process, a three step mechanism (see Fig. 10), $K_{eq}^{ox} = 100$, and $k_f = 30$ s^{-1}.

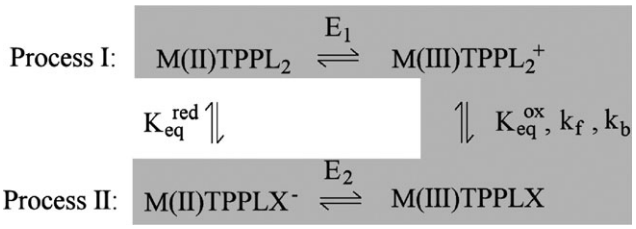

Fig. 10 Schematic representation of the two coupled redox processes with equilibrium steps due to complex formation.

simulated curve at 20 mV s^{-1}, Fig. 9(B)(ii) shows a simulated response at 100 mV s^{-1}, and Fig. 9(B)(iii) shows the expected reversible voltammetric response in the absence of the ion association reaction. The characteristic double peak as well as a shift in peak potential can be reproduced even based on this oversimplified mechanistic model. The use of eqn (6) to establish the apparent equilibrium constant is justified.

In the "square scheme" mechanism in Fig. 10, E_1 and E_2 denote the potentials associated with the reversible oxidation of two distinct metal complexes coupled to anion transfer between aqueous and organic phases, X^- is the anion transferred from the aqueous phase, K_{eq}^{ox} and K_{eq}^{red} are the apparent equilibrium constants for the binding of the anion [which is associated with the removal of one 4-(3-phenylpropyl)pyridine ligand], and k_f and k_b denote rate constants. For the case above (FeTPP, aqueous 0.1 M OCN^-) the apparent equilibrium constant $K_{eq}^{ox} = 100$ and $k_f = 30$ s^{-1}. These values are only "apparent" because the bimolecular nature of the association process and the varying availability of OCN^- in the organic phase are not taken into account in the numerical model. A fuller simulation treatment and better experimental approaches based on porous thin film electrodes[30] are currently under investigation and will be reported in the future.

4. Conclusions

It has been shown that both anion and cation transfer processes are associated with porphyrinato metal complex electrochemistry in organic solvent | water two phase systems. Two phase electrochemical processes provide a new tool and allow processes involving porphyrinato metal complexes to be studied and exploited. In the future, the availability of a range of different porphyrinato metal complexes with different reactivities towards individual anions will allow novel combinatorial microdroplet array approaches to be developed specifically for the detection of certain types or mixtures of anions.

Acknowledgements

Support from Polish–British Partnership Programme sponsored by British Council and Committee for Scientific Research (project WAR/314/248) is gratefully acknowledged.

References

1 H. H. Girault and D. J. Schiffrin, *J. Electroanal. Chem.*, 1989, **15**, 1.
2 J. R. Sandifer, *Ion-transfer kinetics—principles and applications*, VCH, Weinheim, 1995.
3 See for example: W. Schmickler, *Interfacial electrochemistry*, Oxford University Press, Oxford, 1996, p. 153.
4 S. Ulmeanu, H. J. Lee, D. J. Fermin, H. H. Girault and Y. H. Shao, *Electrochem. Commun.*, 2001, **3**, 219.
5 L. Murtomaki and K. Kontturi, *J. Electroanal. Chem.*, 1998, **449**, 225.
6 P. D. Beattie, A. Delay and H. H. Girault, *J. Electroanal. Chem.*, 1995, **380**, 167.
7 B. Kralj and R. A. W. Dryfe, *J. Electroanal. Chem.*, 2003, **560**, 127.
8 C. J. Slevin and P. R. Unwin, *Langmuir*, 1999, **15**, 7361.
9 Z. Samec, N. Eugster, D. J. Fermin and H. H. Girault, *J. Electroanal. Chem.*, 2005, **577**, 323.
10 M. J. Stephenson, S. M. Holmes and R. A. W. Dryfe, *Angew. Chem., Int. Ed.*, 2005, **44**, 3075.
11 H. Tatsumi and H. Katano, *J. Electroanal. Chem.*, 2005, **577**, 59.
12 F. Scholz and U. Hasse, *Electrochem. Commun.*, 2005, **7**, 541.
13 C. Forssten, K. Kontturi, L. Murtomaki, H. C. Hailes and D. E. Williams, *Electrochem. Commun.*, 2001, **3**, 379.
14 F. Marken, C. M. Hayman and P. C. B. Page, *Electrochem. Commun.*, 2002, **4**, 462.
15 J. Y. Chen and M. Sato, *J. Electroanal. Chem.*, 2004, **572**, 153.
16 M. Saczek-Maj and M. Opallo, *Electroanalysis*, 2002, **14**, 1060.
17 F. Scholz, U. Schröder and R. Gulaboski, *Electrochemistry of immobilized particles and droplets*, Springer, Berlin, 2005.
18 T. D. Chung and F. C. Anson, *J. Electroanal. Chem.*, 2001, **508**, 115.
19 C. N. Shi and F. C. Anson, *Anal. Chem.*, 1998, **70**, 3114.
20 C. N. Shi and F. C. Anson, *J. Phys. Chem. B*, 1998, **102**, 9850.
21 S. J. Stott, K. J. McKenzie, R. J. Mortimer, C. M. Hayman, B. R. Buckley, P. C. B. Page, F. Marken, G. Shul and M. Opallo, *Anal. Chem.*, 2004, **76**, 5364.
22 G. Shul, M. Opallo and F. Marken, *Electrochim. Acta*, 2005, **50**, 2315.
23 E. Bak, M. Donten and Z. Stojek, *Electrochem. Commun.*, 2005, **7**, 483.
24 F. Scholz and R. Gulaboski, *Faraday Discuss.*, 2005, **129**, 169.
25 C. E. Banks, T. J. Davies, R. G. Evans, G. Hignett, A. J. Wain, N. S. Lawrence, J. D. Wadhawan, F. Marken and R. G. Compton, *Phys. Chem. Chem. Phys.*, 2003, **5**, 4053.
26 E. Komorsky-Lovric, V. Mirceski, C. Kabbe and F. Scholz, *J. Electroanal. Chem.*, 2004, **566**, 371.
27 F. Quentel, V. Mirceski, M. L'Her, M. Mladenov, F. Scholz and C. Elleouet, *J. Phys. Chem. B*, 2005, **109**, 13228.
28 F. Scholz, R. Gulaboski and K. Caban, *Electrochem. Commun.*, 2003, **5**, 929.
29 F. Marken, K. J. McKenzie, G. Shul and M. Opallo, *Faraday Discuss.*, 2005, **129**, 219.
30 M. A. Ghanem and F. Marken, *Electrochem. Commun.*, 2005, **7**, 1333.
31 See for example: D. T. Sawyer, A. Sobkowiak and J. L. Roberts Jr, *Electrochemistry for chemists*, Wiley, New York, 2nd edn, 1995, p. 470.
32 See for example: D. G. Davis, in *The Porphyrins*, ed. D. Dolphin, Academic Press, London, 1978, vol. 5, p. 127.
33 *Metalloporphyrins in catalytic oxidations*, ed. R. A. Sheldon, Marcel Dekker, New York, 1994.
34 C. N. Shi and F. C. Anson, *Inorg. Chem.*, 1998, **37**, 1037.
35 L. A. Truxillo and D. G. Davis, *Anal. Chem.*, 1975, **47**, 2260.
36 F. Marken, R. D. Webster, S. D. Bull and S. G. Davies, *J. Electroanal. Chem.*, 1997, **437**, 209.
37 Y. Marcus, *Ion Properties*, Marcel Dekker, New York, 1997.
38 U. Schröder, J. Wadhawan, R. G. Evans, R. G. Compton, B. Wood, D. J. Walton, R. R. France, F. Marken, P. C. B. Page and C. M. Hayman, *J. Phys. Chem. B*, 2002, **106**, 8697.
39 M. Rudolph, D. P. Reddy and S. W. Feldberg, *Anal. Chem.*, 1994, **66**, A589.

